

# Stable Fault-Tolerant Adaptive Fuzzy/Neural Control for a Turbine Engine

Yixin Diao and Kevin M. Passino, *Senior Member, IEEE*

**Abstract**—Stimulated by the growing demand for improving the reliability and performance of systems, fault-tolerant control has been receiving significant attention since its goal is to detect the occurrence of faults and achieve satisfactory system performance in the presence of faults. To develop an intelligent fault-tolerant control system, we begin by constructing a design model of the system using a hierarchical learning structure in the form of Takagi–Sugeno fuzzy systems. Afterwards, the fault-tolerant control scheme is designed based on stable adaptive fuzzy/neural control, where its on-line learning capabilities are used to capture the unknown dynamics caused by faults. Finally, the effectiveness of the proposed methods has been studied by extensive analysis of system zero dynamics and asymptotic tracking abilities for both indirect and direct adaptive control cases, and by “component level model” simulation of the General Electric XTE46 turbine engine.

**Index Terms**—Adaptive control, engine, fault-tolerant control, fuzzy systems, neural networks.

## I. INTRODUCTION

MOTIVATED by the growing need for high levels of system performance and reliability in the presence of unexpected changes of system functions, fault-tolerant control is receiving increasing attention. Survey papers by Patton [1] and Stengel [2] present excellent overviews of advances in the research of fault-tolerant control. Due to the complexity and importance of jet engines, the study of fault diagnosis and fault accommodation for jet engines has become a very active research topic for both theoretical and practical reasons. In [3]–[5] the authors studied sensor failure detection for jet engines using a Kalman filter with a generalized likelihood ratio testing based scheme. In [6], [7] the authors derived linearized models of jet engine systems via the  $\alpha$ -canonical form parameterization identification method and applied a parameter estimation approach in fault detection and isolation for the space shuttle main engine. In [8]–[10] the authors studied fault detection of jet engine sensor systems using an eigenstructure assignment technique to design observer based residual generators, and they also studied its robustness. The related reconfigurable flight control problem has been studied for many years and the focus there is to safely recover from structural damage or system faults. In [11] the authors detected

sensor and actuator faults of flight control systems using multiple model adaptive estimation and in [12], [13] a multiple model adaptive control method was used in reconfigurable flight control. In [14] and [15] model following methods were used for a reconfigurable flight control system. In [16] the authors used feedback linearization for restructurable flight control.

Recently, intelligent control has received increasing attention and been applied in the field of nonlinear fault diagnosis and fault-tolerant control (e.g., see the discussion in [17]). The artificial intelligent methods such as fuzzy systems, neural networks and expert systems have the potential to “learn” the plant model from input–output data or “learn” fault knowledge from past experience, and they can be used as function approximators to construct the analytical model for residual generation, or as supervisory schemes to make the fault analysis decisions [18]. The nonlinear modeling ability of neural networks has been utilized for nonlinear fault diagnosis problems [19]–[21]. In addition, the learning ability has also been studied and successfully used in nonlinear robust fault diagnosis [22]–[24]. Meanwhile, expert systems and fuzzy logic have been used in model based fault diagnosis [25]–[30] and in [31] the “fuzzy model reference learning controller,” supervised by an expert system strategy, was used to compensate for actuator failures in an F-16 aircraft.

To develop a fault-tolerant control system we begin by using the CLM (defined in Table I) to generate data that is used by a Levenberg–Marquardt method to train a Takagi–Sugeno fuzzy system to represent the engine (Section II). The resulting nonlinear model provides a reasonably accurate representation of manufacturing differences, engine deterioration, and fault effects. In Section III stable indirect and direct adaptive controllers are applied to achieve fault-tolerant engine control by using Takagi–Sugeno fuzzy systems to “learn” the unknown dynamics caused by faults and to accommodate faults by updating the controller, and this nonlinear model provides *a priori* knowledge about the nominal engine dynamics. We prove that both adaptive schemes achieve asymptotic tracking. In Section IV the performance of the fault-tolerant indirect and direct adaptive controllers is demonstrated through the component level model simulation of the XTE46 engine.

Manuscript received February 3, 2000; revised August 24, 2000. Manuscript received in final form January 26, 2001. Recommended by Associate Editor D. W. Repperger. This work was supported by the NASA Glenn Research Center under Grant NAG3-2084.

Y. Diao is with IBM Thomas J. Watson Research Center, Hawthorne, NY 10532 USA.

K. M. Passino is with the Department of Electrical Engineering, Ohio State University, Columbus, OH 43210 USA (e-mail: passino@ee.eng.ohio-state.edu).

Publisher Item Identifier S 1063-6536(01)03362-0.

## II. MODEL DEVELOPMENT USING TAKAGI–SUGENO FUZZY SYSTEMS

### A. The XTE46 Turbine Engine

The General Electric XTE46 engine, as shown in Fig. 1, is a simplified, unclassified version of the original IHPTET engine [32]. To develop a fault-tolerant engine controller an accurate

TABLE I  
TABLE OF ACRONYMS

\*

CLM	Component Level Model
XNL	Fan rotor speed
XNH	Core rotor speed
TMPC	Temperature at combustor inlet
ALT	Altitude
XM	Mach number
PC	Power code
WF36	Combustor fuel flow
A8	Exhaust nozzle area
A16	Variable area bypass injector area
ZSW2	Fan flow
SEDM2	Fan efficiency
ZSW7D	Compressor tip flow
SEDM7D	Compressor tip efficiency
ZSW27	Compressor hub flow
SEDM27	Compressor hub efficiency
ZSW41	High pressure turbine flow
ZSE41	High pressure turbine efficiency
ZSW49	Low pressure turbine flow
ZSE49	Low pressure turbine efficiency

representation of the engine dynamics is desired. This model may be used as the “truth model” (or “design model”) in the control simulation to represent the real engine, or may serve as the nominal model (known dynamics) in a “model-based” control strategy. However, modeling a turbine engine is undoubtedly a very difficult problem due to the fact that the jet engine system has an iterative structure, which means that the model cannot be written down in a differential-algebraic equation form. Fortunately, a thermodynamic simulation package, the component level engine cycle model (CLM) of the XTE46 engine, was provided by General Electric Aircraft Engines (GEAE). This is a sophisticated, highly nonlinear dynamic model where each engine component is simulated. The CLM executes one pass within the digital control’s sampling time and thermodynamic states are assumed to be in equilibrium after each pass through the simulation. The CLM is a low-frequency transient turbofan engine simulation, and volume dynamics and airflow storage effects, which are high frequency phenomena, are not included. The operating condition of the engine is defined by the altitude (ALT), the mach number (XM), the difference of temperature (DTAMB) and the throttle setting represented by power code (PC). The health of the engine is described by ten quality parameters which include the

flows and efficiencies of the fan (ZSW2 and SEDM2), the compressor (ZSW7D, SEDM7D, ZSW27, and SEDM27), and turbines (ZSW41, ZSE41, ZSW49, and ZSE49). The model has three state variables, including the fan rotor speed (XNL), the core rotor speed (XNH) and the temperature at combustor inlet (TMPC). There are six actuators, but the major control variables are the combustor fuel flow (WF36), the exhaust nozzle area (A8), and the variable area bypass injector area (A16).

From the point of view of theoretical studies in fault-tolerant control, the component level model is too complicated. Although the CLM does provide a driver to trim the model to specified operating conditions and generate linearized models, studies show that the accuracy of the linear models is not adequate for our purposes (where we consider faults with significant nonlinear effects). Here, we developed a nonlinear model with Takagi–Sugeno fuzzy systems using a system identification methodology that utilized nonlinear transient data generated by the CLM. This model will be used for theoretical studies (i.e., building the stable adaptive controller), for representing the dynamics of nominal engine (as “known” system dynamics in the indirect adaptive controller), and for preliminary simulation studies (i.e., it serves as the truth model of the engine).

### B. The Takagi–Sugeno Fuzzy System

Developing mathematical models for nonlinear systems can be quite challenging. Takagi–Sugeno fuzzy systems are capable of serving as the analytical model for nonlinear systems due to the universal approximation property, that is, any desired approximation accuracy can be achieved by increasing the size of the approximation structure and properly defining the parameters of the approximator [33]. A Takagi–Sugeno fuzzy system can be defined by

$$y = F_{ts}(x, \theta) = \frac{\sum_{i=1}^R g_i(x) \mu_i(x)}{\sum_{i=1}^R \mu_i(x)} \quad (1)$$

$$g_i(x) = a_{i,0} + a_{i,1}x_1 + \cdots + a_{i,n}x_n \quad (2)$$

$$\mu_i(x) = \prod_{j=1}^n \exp\left(-\frac{1}{2} \left(\frac{x_j - c_j^i}{\sigma_j^i}\right)^2\right) \quad (3)$$

where

$$\begin{array}{ll} y & \text{output of the fuzzy system;} \\ x = [x_1, x_2, \dots, x_n]^T & \text{holds the } n \text{ inputs;} \\ i = 1, 2, \dots, R & R \text{ different rules.} \end{array}$$

The shapes of the membership functions are chosen to be Gaussian, and center-average defuzzification and product are used for the premise and implication in the structure of the fuzzy system. The  $g_i(x)$ ,  $i = 1, 2, \dots, R$  are called consequent functions of the fuzzy system, where the  $a_{i,j}$  are constants. The premise membership functions  $\mu_i(x)$  are assumed to be well defined so that  $\sum_{i=1}^R \mu_i(x) \neq 0$  for all  $x$ . The parameters that enter in a nonlinear fashion are  $c_j^i$  and  $\sigma_j^i$ , which are the centers and relative widths of the membership functions,

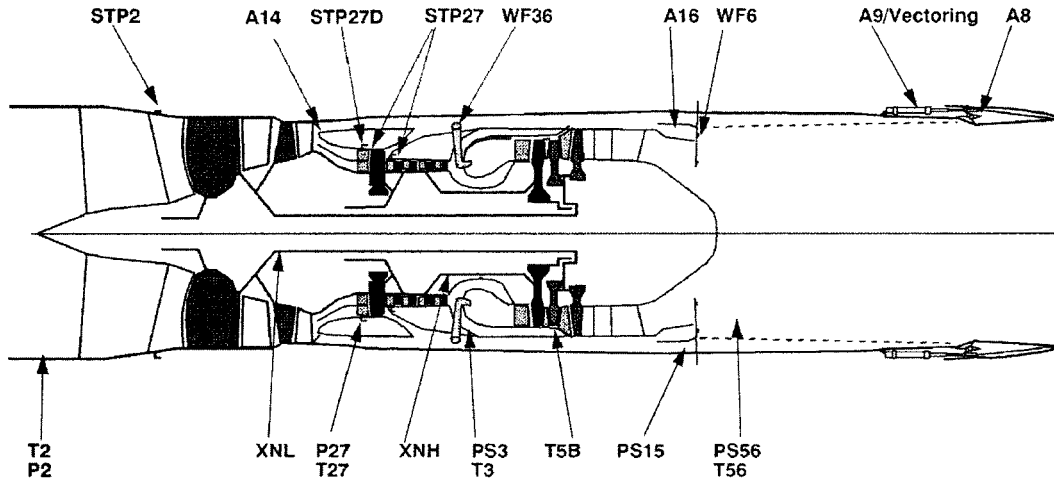


Fig. 1. Schematic of the XTE46 turbine engine.

respectively, for the  $j$ th inputs and the  $i$ th rules. Actually, the Takagi–Sugeno fuzzy system, where the consequent parts are chosen to be affine functions, is a special case of “functional fuzzy systems” [33]. If other functions such as polynomials or neural networks are used as consequent functions, different kinds of functional fuzzy systems will be generated.

The tunable parameter vector  $\theta$  in (1) can be composed of both premise membership function parameters ( $c_j^i$  and  $\sigma_j^i$ ) and consequent function parameters ( $a_{i,j}$ ). This is referred to as *nonlinear in the parameter* case. A *nonlinear in the parameter* Takagi–Sugeno fuzzy system can be tuned by a variety of gradient methods such as the steepest descent method and Levenberg–Marquardt method. Alternatively, the parameter vector  $\theta$  may be composed of only the consequent function parameters so that  $y$  is a linear function of  $\theta$ . To tune the fuzzy approximator for this *linear in the parameter* case, a linear least squares method will normally be suitable.

### C. Fuzzy Modeling for the XTE46 Engine

The CLM for the XTE46 aircraft engine is a complicated multiple-input multiple-output (MIMO) nonlinear system (involving schedules, look-up tables, and partial differential equations). However, GE Aircraft Engines (the authority on this engine) indicates that the key single-input single-output (SISO) loop (i.e., fuel flow to fan speed loop) is not tightly coupled with other loops. Therefore, to focus our theoretical studies, we could assume that the fundamental engine dynamic characteristics of interest are represented by a SISO system (while the other two input variables A8 and A16 could be properly scheduled as functions of the power level and the inlet temperature). The SISO nonlinear system is in the form

$$\dot{x} = f(x, u, c, p) \quad (4)$$

$$y = h(x, u, c, p) \quad (5)$$

where  $x = [\text{XNL}, \text{XNH}, \text{TMPC}]^T$  is the state vector,  $u = \text{WF36}$  is the input variable,  $y = \text{XN2}$  is the output of the engine,  $c = [\text{ALT}, \text{XM}, \text{DTAMB}, \text{PC}]^T$  represents the operating condition of the engine, and  $p = [\text{ZSW2}, \text{SEDM2}, \text{ZSW7D}, \text{SEDM7D}, \text{ZSW27}, \text{SEDM27},$

$\text{ZSW41}, \text{ZSE41}, \text{ZSW49}, \text{ZSE49}]^T$  represents the quality parameter vector. The function  $f(\cdot)$  denotes the unknown function representing the nonlinear characteristics of the engine, and  $h(\cdot) = \text{XNL}$  because the output variable XN2 is the measurement of the state variable XNL.

The analytical model of the engine is developed in two steps. Fuzzy identification is applied first to generate (a grid of) “node” models specified by operating conditions and quality parameters. Afterwards, the “global” model can be constructed by fuzzy interpolation on these node models. (We use this two-step method rather than identifying the model directly from the data collected from the whole space of operating conditions and quality parameters in that it is practically impossible to train an approximator using such a large amount of data, due to the limitations of computing resources.) Given a specific operating condition ( $c_i$ ) and fixed values of quality parameters ( $p_i$ ), the node model for the XTE46 engine can be obtained using nonlinear identification techniques as

$$\widehat{\text{XNLdot}}(k) = F_{ts}^1(\widehat{\text{XNL}}(k), \widehat{\text{XNH}}(k), \text{WF36}(k), \theta^1(c_i, p_i)) \quad (6)$$

$$\widehat{\text{XNHdot}}(k) = F_{ts}^2(\widehat{\text{XNL}}(k), \widehat{\text{XNH}}(k), \text{WF36}(k), \theta^2(c_i, p_i)) \quad (7)$$

$$\widehat{\text{XNL}}(k+1) = \widehat{\text{XNL}}(k) + T_s \widehat{\text{XNLdot}}(k) \quad (8)$$

$$\widehat{\text{XNH}}(k+1) = \widehat{\text{XNH}}(k) + T_s \widehat{\text{XNHdot}}(k) \quad (9)$$

$$\widehat{\text{XN2}}(k+1) = \widehat{\text{XNL}}(k+1) \quad (10)$$

where two multiple-input single-output (MISO) Takagi–Sugeno fuzzy systems,  $F_{ts}^1$  and  $F_{ts}^2$ , are specified with corresponding parameters  $\theta^1$  and  $\theta^2$ , respectively. The variables  $\widehat{\text{XNL}}(k)$  and  $\widehat{\text{XNH}}(k)$  denote the estimated values of  $\text{XNL}(k)$  and  $\text{XNH}(k)$  [where  $\widehat{\text{XNL}}(0) = \text{XNL}(0)$  and  $\widehat{\text{XNH}}(0) = \text{XNH}(0)$  to let the fuzzy model have the same initial values as the engine]. The variable  $\widehat{\text{XN2}}(k)$  is the estimated value of  $\text{XN2}(k)$ . The variables  $\widehat{\text{XNLdot}}(k)$  and  $\widehat{\text{XNHdot}}(k)$  are the outputs of the fuzzy systems, and  $T_s$  is the sample time, which is 0.02 s. The fuzzy systems are trained using engine data generated by the transient

driver of the component level model simulator of the XTE46 engine. One thousand engine input-output data pairs are collected which reflect the transient performance of the engine for 20 s (sampled every 0.02 s) at a specific “node” (of operating conditions and quality parameters). For the  $k$ th experimental data pair, the input data are the state variables  $XNL(k)$  and  $XNH(k)$  and the input variable  $WF36(k)$ . The output data are  $XNLdot(k)$  and  $XNHdot(k)$ , which denote the derivatives of  $XNL(k)$  and  $XNH(k)$ , respectively.

The structure of the fuzzy approximators is specifically selected to satisfy the requirement of stable adaptive control [it should be affine, i.e., in the form of  $\dot{x} = f(x) + g(x)u$ , for the sake of feedback linearization]. In particular, the premise input is chosen to be  $\widehat{XNL}(k)$  only so that the Takagi–Sugeno fuzzy system can be written in the affine form as

$$\begin{aligned} & F_{ts}(\widehat{XNL}(k), \widehat{XNH}(k), WF36(k), \theta) \\ &= \frac{\sum_{j=1}^R (a_{j,0} + a_{j,1}\widehat{XNL}(k) + a_{j,2}\widehat{XNH}(k))\mu_j(\widehat{XNL}(k))}{\sum_{j=1}^R \mu_j(\widehat{XNL}(k))} \\ &+ \frac{\sum_{j=1}^R a_{j,3}\mu_j(\widehat{XNL}(k))}{\sum_{j=1}^R \mu_j(\widehat{XNL}(k))} WF36(k). \end{aligned}$$

Actually, we could use either one of the state variables as the input of the premise membership functions (to divide the nonlinear space into several fuzzy regions) because the fan rotor speed ( $XNL$ ) and the core rotor speed ( $XNH$ ) are quite correlated to each other. Here, we choose  $\widehat{XNL}$  to be the premise input for the reason to simplify the analysis of system “zero dynamics” in the following section.

Using trial and error, three rules were selected for each fuzzy model, and these models were tuned by a Levenberg–Marquardt method using data collected at each node. Notice that we did not use TMPC as one of the model inputs (it is not measurable) and it is not necessary to estimate TMPC either because we found that the importance of TMPC to the model accuracy is trivial. This is verified by an input selection method referred to as “regressor analysis” (where a regression model is constructed and the regression coefficients are analyzed to determine the importance of each input).

Also note that this nonlinear engine model is running in an “open-loop manner,” that is, the outputs of the model will be fed back into the model as the inputs (which is referred to as a parallel model). This implies that it will become more difficult to construct such a model (compared to directly using the engine states as the inputs of the model) and only basic behaviors of the engine may be obtained due to the drifting effects caused by the accumulation of approximation errors. However, we prefer to use this approach because we want to generate a design model capable of characterizing the system dynamics so

that we can design the adaptive controller based on it. In addition, sometimes we want this model to be running as the “truth engine” in the simulation studies (before we apply the controller to the real engine), where the CLM and thus the engine states  $XNL$  and  $XNH$  are not available. Of course, when we utilize the model (e.g., as the known dynamics of the nominal engine in our fault-tolerant controller) to control the CLM, we may use the (measurable) real engine states to be the inputs of fuzzy systems and may expect an improvement in model accuracy.

By nonlinearly interpolating between a grid of node models obtained above from nonlinear system identification, the regional model can be constructed which is in the form of

$$\begin{aligned} & \widehat{XNLdot}(k) \\ &= \frac{\sum_{i=1}^N F_{ts}^1(\widehat{XNL}(k), \widehat{XNH}(k), WF36(k), \theta^1(c_i, p_i))\mu_i(z)}{\sum_{i=1}^N \mu_i(z)} \\ & \widehat{XNHdot}(k) \\ &= \frac{\sum_{i=1}^N F_{ts}^2(\widehat{XNL}(k), \widehat{XNH}(k), WF36(k), \theta^2(c_i, p_i))\mu_i(z)}{\sum_{i=1}^N \mu_i(z)} \end{aligned}$$

$$\mu_i(z) = \prod_{j=1}^{14} \exp\left(-\frac{1}{2} \left(\frac{z_j - c_j^i}{\sigma_j^i}\right)^2\right)$$

where  $i = 1, 2, \dots, N$  represent  $N$  different models and  $z = [c^T, p^T]^T$  is the premise input vector including 14 variables representing operating conditions and quality parameters.

We choose to focus on fault-tolerant controller development for the “climb” region (which is defined as  $ALT \in [12500, 17500]$ ,  $XM \in [0.6, 0.8]$ ,  $DTAMB \in [-35, 35]$ , and  $PC \in [45, 50]$ ). We partition each operating condition variable into three regions to define our grid. In this way, we have  $3^4 = 81$  models to describe the nonlinearity presented in the climb region. The values of quality parameters ( $p = p_0 + p_{iev} + p_d + p_f$ ) are composed of four parts: the nominal value ( $p_0 = 1$ ), the initial engine variation due to manufacturing differences ( $p_{iev}$ ), the quality parameter adjustment resulted from engine deterioration ( $p_d$ ), and the quality parameter change due to the faults ( $p_f$ ). Note that the effects of engine deterioration and faults are larger than the initial engine variation, so that we would like to capture the characteristics of these two major factors and leave the effects of initial engine variation to be model uncertainty. By assuming that the engine deterioration affects ten quality parameters in the same way, we could use a deterioration index  $I_d$  to describe its effects and may have three grids to represent no deterioration ( $I_d = 0$ ), half deterioration ( $I_d = 0.5$ ), and full deterioration ( $I_d = 1$ ), respectively. Furthermore, we consider four different sizes of faults, that is, no fault (the corresponding variable in  $p_f$  is 0), small fault (the corresponding variable in  $p_f$  is

−1%), medium fault (the corresponding variable in  $p_f$  is −2%), and large fault (the corresponding variable in  $p_f$  is −3%). For example, a small fan fault is characterized by  $p_{f,ZSW2} = -1\%$  and  $p_{f,SEDM2} = -1\%$ , where ZSW2 and SEDM2 are the engine quality parameters reflecting the flow and efficiency of the fan, respectively, which will be degraded after the occurrence of the fan fault. Note that here we only consider the “local” fault, that is, only the physical characteristics (and thus the flow and efficiency parameters) of the corresponding engine component are affected. For instance, if a large compressor hub fault occurs, it will affect the flow ( $p_{f,ZSW27} = -3\%$ ) and efficiency ( $p_{f,SEDM27} = -3\%$ ) of the compressor hub accordingly, but have no effects on the flow ( $p_{f,ZSW2} = 0\%$ ) and efficiency ( $p_{f,SEDM2} = 0\%$ ) of the fan.

As a result, we have  $3 \times 4 \times 4 = 48$  models to describe the nonlinearity presented in the quality parameters (for simplicity, here we only consider two possible faults: fan fault and compressor hub fault). In total, we have  $81 \times 48 = 3888$  (nonlinear) node models to describe the nonlinearity in the climb region. We need this level of complexity to obtain a reasonably accurate “design model” for the development of our controller.

The general form of the model can be described as

$$\dot{x} = f(x, c, p) + g(x, c, p)u \quad (11)$$

where

$$f(x, c, p) = \frac{\sum_{i=1}^N \underline{f}(x, c_i, p_i) \mu_i(c, p)}{\sum_{i=1}^N \mu_i(c, p)}$$

$$g(x, c, p) = \frac{\sum_{i=1}^N \underline{g}(x, c_i, p_i) \mu_i(c, p)}{\sum_{i=1}^N \mu_i(c, p)}$$

$$\underline{f}(x, c_i, p_i) = \frac{\sum_{j=1}^R [a_{j,0}(c_i, p_i) + a_{j,1}(c_i, p_i)x_1] \underline{\mu}_j(x_1)}{\sum_{j=1}^R \underline{\mu}_j(x_1)} + \frac{\sum_{j=1}^R a_{j,2}(c_i, p_i)x_2 \underline{\mu}_j(x_1)}{\sum_{j=1}^R \underline{\mu}_j(x_1)}$$

$$\underline{g}(x, c_i, p_i) = \frac{\sum_{j=1}^R a_{j,3}(c_i, p_i) \underline{\mu}_j(x_1)}{\sum_{j=1}^R \underline{\mu}_j(x_1)}$$

where  $u = \text{WF36}$  is the system input (fuel flow), and  $x = [x_1, x_2]^T = [\widehat{\text{XNL}}, \widehat{\text{XNH}}]^T$  represents the system states (fan speed and core speed), which is positive since the speed cannot be negative and  $x \in S_x$  (a valid speed region). The value of  $c$  is the known operating condition vector,  $p$  is unknown quality parameter vector, and  $c_i$  and  $p_i$  specify the nodes where we establish the local models. Also,  $f = [f_1, f_2]^T$  and  $g = [g_1, g_2]^T$  are  $2 \times 1$  function vectors obtained through fuzzy interpolation, and  $\mu_i(c, p)$  are interpolating membership functions. Moreover,  $\underline{f} = [\underline{f}_1, \underline{f}_2]^T$  and  $\underline{g} = [\underline{g}_1, \underline{g}_2]^T$  are  $2 \times 1$  function vectors obtained through nonlinear system identification and are in the form of Takagi–Sugeno fuzzy systems, where  $a_{j,0}$ ,  $a_{j,1}$ ,  $a_{j,2}$ , and  $a_{j,3}$  are  $2 \times 1$  parameter vectors of the (linear) consequent functions, and  $\underline{\mu}_j(x_1)$  are membership functions describing local nonlinearity with respect to  $x_1$ .

By inspecting the parameters that result from the identification process we found that  $a_{j,3}^1(c_i, p_i) > a_{j,3}^2(c_i, p_i) > 0$  and  $a_{j,2}^2(c_i, p_i) < a_{j,2}^1(c_i, p_i) < 0$  for any  $i = 1, 2, \dots, N$ ,  $j = 1, 2, \dots, R$ . Basically, these sign conditions explain some physical dynamics of the engine. In particular, the relationships among the state variables and the input variable are relevant for stability analysis of the system. For instance, we have both  $a_{j,3}^1(c_i, p_i) > 0$  and  $a_{j,2}^2(c_i, p_i) > 0$ , which indicate that if the fuel flow is increased, both the fan rotor speed and the core rotor speed will be increased. These constraints on the model parameters are important to design and analyze the stable adaptive control system. For example, by knowing  $a_{j,3}^1(c_i, p_i) > 0$  for any operating conditions and quality parameters [and  $\underline{\mu}_j(x_1) > 0$  and  $\sum_{j=1}^R \underline{\mu}_j(x_1) \neq 0$  by the definition of Takagi–Sugeno fuzzy systems], we obtain  $\underline{g}^1(x, c_i, p_i) > 0$  and thus  $g_1(x, c, p) > 0$  for all  $x, c, p$ . This implies the “relative degree” of the engine is one (which we will discuss later). In addition, more details on how to use these relationships to determine the system zero dynamics will also be provided in the stability analysis part of the following section.

The resulting nonlinear model provides a reasonably accurate representation of engine dynamics (GE Aircraft Engines verified this for us). Here we give an example at a point different from the nodes where we generated the model. The engine operating conditions are ALT = 16 000, XM = 0.75, DTAMB = 0, and PC = 46. The quality parameters are defined by considering some initial engine variation, nearly half engine deterioration ( $I_d = 0.4$ ), and a fan fault a little bit larger than medium size ( $p_{f,ZSW2} = -2.2\%$  and  $p_{f,SEDM2} = -2.2\%$ ). Fig. 2 compares system responses between the nonlinear model and the CLM and indicates their similarity (where the solid lines represent the system response of the CLM and the dashed lines represent that of the analytical model). We also conducted many other such simulations to verify the quality of our design model; however, in the interest of brevity we do not include those plots here.

### III. FAULT-TOLERANT STABLE ADAPTIVE FUZZY/NEURAL CONTROL

In this section we will develop fault-tolerant engine control using stable adaptive fuzzy/neural controllers [34]. Both indirect and direct adaptive control approaches are applied. We also

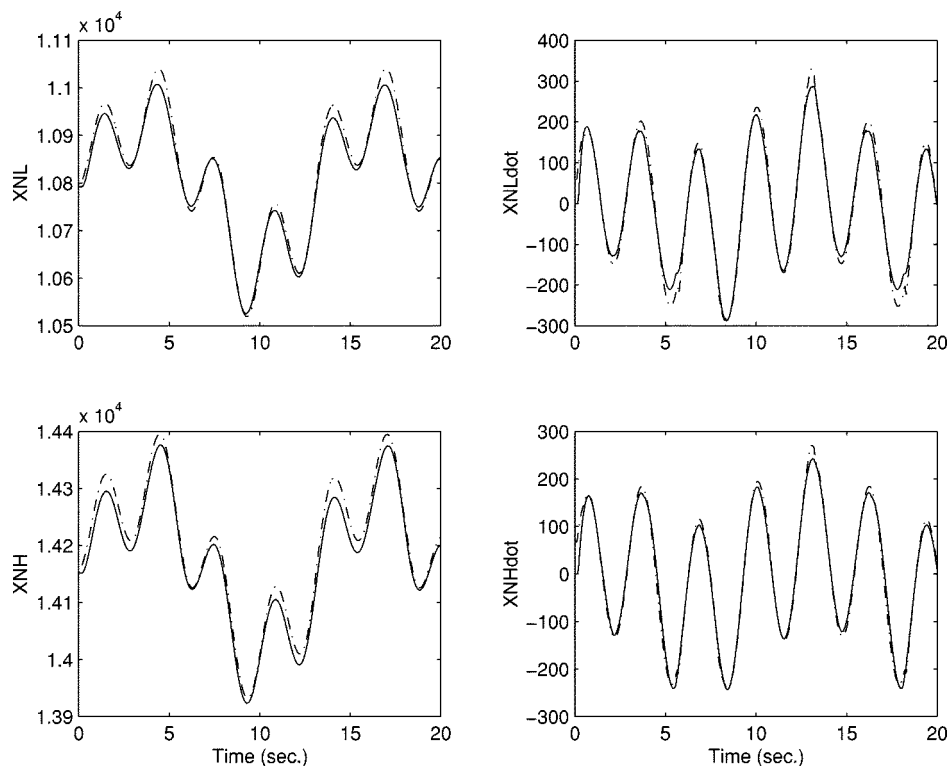


Fig. 2. Illustrative example of the model performance.

show that under certain conditions asymptotic tracking of a reference signal and boundedness of all signals are achieved.

#### A. Indirect Adaptive Control

The general framework for modeling the nonlinear SISO system with various faults is described by the differential equation

$$\dot{x} = f(x) + g(x)u \quad (12)$$

$$y = h(x) \quad (13)$$

where

$x = [x_1, x_2, \dots, x_n]^T$  state vector;  
 $u$  (scalar) input;  
 $y$  (scalar) output of the system;  
 functions  $f(x)$ ,  $g(x)$  which are smooth, represent both the nominal system dynamics and any change of system due to a fault.

Let  $L_g^d h(x)$  be the  $d$ th Lie derivative of  $h(x)$  with respect to  $g(x)$  [i.e.,  $L_g h(x) = (\partial h / \partial x)^T g(x)$ ,  $L_g^2 h(x) = L_g(L_g h(x)) = (\partial((\partial h / \partial x)^T g(x)) / \partial x)^T g(x)$ , etc.]. A system is said to have “strong relative degree”  $d$  if  $L_g h(x) = L_g L_f h(x) = \dots = L_g L_f^{d-2} h(x) = 0$  and  $L_g L_f^{d-1} h(x) \neq 0$  for all  $x$ . If system (12), (13) has strong relative degree  $d$ , then

$$\dot{\xi}_1 = \xi_2 = L_f h(x)$$

$$\dot{\xi}_2 = \xi_3 = L_f^2 h(x)$$

$\vdots$

$$\begin{aligned} \dot{\xi}_{d-1} &= \xi_d = L_f^{d-1} h(x) \\ \dot{\xi}_d &= L_f^d h(x) + L_g L_f^{d-1} h(x)u \end{aligned}$$

with  $\xi_1 = y$ , which, if we let  $y^{(d)}$  denote the  $d$ th derivative of  $y$ , may be rewritten as

$$y^{(d)} = [\alpha_k(t) + \alpha(x)] + [\beta_k(t) + \beta(x)]u \quad (14)$$

where  $\alpha_k(t)$  and  $\beta_k(t)$  are “known” dynamics of the system (e.g., the nominal model dynamics) that may depend on the states or known exogenous time dependent signals (which may represent the time profile of faults identified from the fault diagnosis scheme), and  $\alpha(x)$  and  $\beta(x)$  represent nonlinear dynamics of the plant that are unknown. Note that here we represent the relationship between known and unknown dynamics to be additive for the convenience of analysis but the actual relationship is not required to be additive. This is because no matter what kinds of systems we consider and what parts of the dynamics are assumed to be known, the unknown dynamics ( $f_u$ ) can always be represented as the difference between the whole system dynamics ( $f$ ) and the known system dynamics ( $f_k$ ), that is,  $f_u = f - f_k$ .

For the purpose of stability analysis we assume that for some  $\beta_0 > 0$ , we have  $|\beta_k(t) + \beta(x)| \geq \beta_0$  so that it is always bounded away from zero [for convenience we further assume that  $\beta_k(t) + \beta(x) \geq 0$ , however, the following analysis may easily be modified for systems which are defined with  $\beta_k(t) + \beta(x) \leq 0$ ]. We also assume that if  $x$  is bounded, then  $\alpha_k(t)$  and  $\beta_k(t)$  are bounded. For our engine application, we will use analytical studies on our model to specify a value for  $\beta_0$ .

The on-line approximators are used to learn the unknown dynamics comprising modeling errors and system changes due to

faults so as to achieve fault accommodation. We may choose radial basis function neural networks, B-spline neural networks, Takagi–Sugeno fuzzy systems or other *linear in the parameter* approximators so that the approximations of  $\alpha(x)$  and  $\beta(x)$  of the actual system are

$$\hat{\alpha}(x) = \theta_\alpha^\top(t) \phi_\alpha(x) \quad (15)$$

$$\hat{\beta}(x) = \theta_\beta^\top(t) \phi_\beta(x) \quad (16)$$

where the vectors  $\theta_\alpha(t)$  and  $\theta_\beta(t)$  are updated on line and are assumed to be defined within the compact parameter sets  $\Omega_\alpha$  and  $\Omega_\beta$ , respectively. In addition, we define the subspace  $S_x \subseteq \mathbb{R}^n$  as the space through which the state trajectory may travel under closed-loop control (we are making no *a priori* assumptions here about the size of  $S_x$ ). We also define

$$\alpha(x) = \theta_\alpha^{*\top} \phi_\alpha(x) + \omega_\alpha(x) \quad (17)$$

$$\beta(x) = \theta_\beta^{*\top} \phi_\beta(x) + \omega_\beta(x) \quad (18)$$

where

$$\theta_\alpha^* = \arg \min_{\theta_\alpha \in \Omega_\alpha} \left( \sup_{x \in S_x} |\theta_\alpha^\top \phi_\alpha(x) - \alpha(x)| \right) \quad (19)$$

$$\theta_\beta^* = \arg \min_{\theta_\beta \in \Omega_\beta} \left( \sup_{x \in S_x} |\theta_\beta^\top \phi_\beta(x) - \beta(x)| \right) \quad (20)$$

are the optimal parameters and  $\omega_\alpha(x)$  and  $\omega_\beta(x)$  are approximation errors which arise when  $\alpha(x)$  and  $\beta(x)$  are represented by finite size approximators. We assume that

$$|\omega_\alpha(x)| \leq W_\alpha(x) \quad (21)$$

$$|\omega_\beta(x)| \leq W_\beta(x) \quad (22)$$

where  $W_\alpha(x)$  and  $W_\beta(x)$  are known state dependent bounds on the error in representing the actual system with approximators (which are, actually, treated as design parameters and tuned when we design the adaptive controller). We also define parameter errors to be

$$\tilde{\theta}_\alpha(t) = \theta_\alpha(t) - \theta_\alpha^* \quad (23)$$

$$\tilde{\theta}_\beta(t) = \theta_\beta(t) - \theta_\beta^* \quad (24)$$

We view fault-tolerant control to be a tracking problem, that is, to design a control system which will cause the output  $y(t)$  and its derivatives  $\dot{y}(t), \dots, y^{(d)}(t)$  to track a desired reference trajectory  $y_m(t)$  and its derivatives  $\dot{y}_m(t), \dots, y_m^{(d)}(t)$ , respectively, which we assume to be bounded. The reference trajectory may be defined by a reference signal whose first  $d$  derivatives may be measured, or by any reference input  $r(t)$  passing through a reference model, with relative degree equal to or greater than  $d$ . In particular, a linear reference model may be

$$\frac{Y_m(s)}{R(s)} = \frac{q(s)}{p(s)} = \frac{q_0}{s^d + p_{d-1}s^{d-1} + \dots + p_0} \quad (25)$$

where  $p(s)$  is the pole polynomial with stable roots.

The indirect adaptive control law

$$u = u_{ce} + u_{si} \quad (26)$$

is comprised of a ‘‘certainty equivalence’’ control term  $u_{ce}$  and a ‘‘sliding mode’’ control term  $u_{si}$ . Let the tracking error be  $e(t) = y_m(t) - y(t)$  and a measure of the tracking error be  $e_s(t) = e^{(d-1)}(t) + k_{d-2}e^{(d-2)}(t) + \dots + k_1\dot{e}(t) + k_0e(t)$ , that is, in the frequency domain,  $e_s(s) = L(s)e(s)$  with  $L(s) = s^{(d-1)} + k_{d-2}s^{(d-2)} + \dots + k_1s + k_0$  whose roots are chosen to be in the (open) left half plane. Also, for convenience below we let  $\bar{e}_s(t) = \dot{e}_s(t) - e^{(d)}(t)$ . Notice that our control goal is to drive  $e_s(t) \rightarrow 0$  as  $t \rightarrow \infty$  and the shape of the error dynamics is dictated by the choice of the design parameters in  $L(s)$ .

The certainty equivalence control term is defined as

$$u_{ce} = \frac{1}{\beta_k(t) + \hat{\beta}(x)} (-\alpha_k(t) + \hat{\alpha}(x) + \nu(t)) \quad (27)$$

where  $\beta_k(t) + \hat{\beta}(x)$  is bounded away from zero (which will be ensured later using projection) so that  $u_{ce}$  is well defined, and

$$\nu(t) = y_m^{(d)} + \eta e_s + \bar{e}_s \quad (28)$$

with  $\eta > 0$  as a design parameter. Consider the update laws

$$\dot{\theta}_\alpha(t) = -Q_\alpha^{-1} \phi_\alpha(x) e_s \quad (29)$$

$$\dot{\theta}_\beta(t) = -Q_\beta^{-1} \phi_\beta(x) e_s u_{ce} \quad (30)$$

where  $Q_\alpha$  and  $Q_\beta$  are positive definite and diagonal and serve as adaptation gains for the parameter updates. Note that the above adaptation laws do not guarantee that  $\theta_\alpha \in \Omega_\alpha$  and  $\theta_\beta \in \Omega_\beta$  so that we will use a projection method to ensure this, in particular, to make sure that  $\beta_k(t) + \hat{\beta}(x) \geq \beta_0$ . Additionally, the sliding mode control term is defined as

$$u_{si} = \frac{(W_\alpha(x) + W_\beta(x)|u_{ce}|)}{\beta_0} \text{sgn}(e_s). \quad (31)$$

## B. Stability Analysis

It is of particular interest to study the zero dynamics of the system with relative degree  $d < n$  to achieve state boundedness. The dynamics for a relative degree  $d$  system described by (12), (13) may be written in normal form as

$$\dot{\xi}_1 = \xi_2 \quad (32)$$

$$\dot{\xi}_2 = \xi_3 \quad (33)$$

⋮

$$\dot{\xi}_{d-1} = \xi_d \quad (34)$$

$$\dot{\xi}_d = \alpha(\xi, \pi) + \beta(\xi, \pi)u \quad (35)$$

$$\dot{\pi} = f_0(\xi, \pi) \quad (36)$$

with  $\xi \in \mathbb{R}^d$ ,  $\pi \in \mathbb{R}^{n-d}$ , and  $y = \xi_1$ . This transformation of the model form can be taken by a change of variables

$$z = T(x) = \begin{bmatrix} \psi_1(x) \\ \vdots \\ \psi_d(x) \\ \cdots \\ \phi_1(x) \\ \vdots \\ \phi_{n-d}(x) \end{bmatrix} = \begin{bmatrix} \psi(x) \\ \phi(x) \end{bmatrix} = \begin{bmatrix} \xi \\ \pi \end{bmatrix} \quad (37)$$

where  $\psi_1(x) = h(x)$ ,  $\psi_{i+1}(x) = (\partial\psi_i/\partial x)^\top f(x)$ ,  $i = 1, 2, \dots, d-1$  and  $(\partial\phi_j/\partial x)^\top g(x) = 0$ ,  $j = 1, 2, \dots, n-d$  for any  $x \in D_x$ , and  $T(x)$  is a diffeomorphism on a domain  $D_x \subset S_x$  [The map  $T$  is invertible and both  $T(\cdot)$  and  $T^{-1}(\cdot)$  are continuously differentiable];  $[\ ]$  shows the existence of  $\phi(x)$  and  $T(x)$ . The normal form decomposes the system states into an external part  $\xi$  and an internal part  $\pi$ . The external part is stabilized by the control  $u$  (which we will show later), while the internal part is made unobservable by the same control. Note that by having  $\xi = 0$  in the inner part we obtain the ‘‘zero dynamics’’ of the system

$$\dot{\pi} = f_0(0, \pi). \quad (38)$$

In particular, if the origin ( $\xi = 0$ ,  $\pi = 0$ ) is an equilibrium point, the exponential stability of zero dynamics may be studied around the origin. Actually, the zero dynamics can be characterized in the original  $x$ -coordinates [1]. Notice that keeping the output identically zero ( $y = 0$ ) gives  $\xi = 0$ , which implies that the solution of the state equation must be confined to the set

$$z^* = \{x \in S_x : \psi_1(x) = \psi_2(x) = \cdots = \psi_d(x) = 0\} \quad (39)$$

and keeping the output identically zero also gives

$$u = u^*(x) = \frac{-\alpha(\xi, \pi) + k\xi}{\beta(\xi, \pi)} \quad (40)$$

so that the zero dynamics in the original  $x$ -coordinates are

$$\dot{x} = f^*(x) = f(x) + g(x)u|_{x \in z^*, u = u^*(x)}. \quad (41)$$

Consider the model of the engine

$$\dot{x}_1 = f_1(x, c, p) + g_1(x, c, p)u \quad (42)$$

$$\dot{x}_2 = f_2(x, c, p) + g_2(x, c, p)u \quad (43)$$

$$y = x_1. \quad (44)$$

To simplify the stability analysis we change the variables  $x_1 = \bar{x}_1 + x_1^0$ ,  $x_2 = \bar{x}_2 + x_2^0$ ,  $u = \bar{u} + u^0$ ,  $y = \bar{y} + x_1^0$  to transform the engine model to the form of

$$\begin{aligned} \dot{\bar{x}}_1 &= [f_1(\bar{x} + x^0, c, p) + g_1(\bar{x} + x^0, c, p)u^0] \\ &\quad + g_1(\bar{x} + x^0, c, p)\bar{u} \\ \dot{\bar{x}}_2 &= [f_2(\bar{x} + x^0, c, p) + g_2(\bar{x} + x^0, c, p)u^0] \\ &\quad + g_2(\bar{x} + x^0, c, p)\bar{u} \end{aligned}$$

so that the above system has an open-loop equilibrium at the origin, that is,  $f_1(x^0, c, p) + g_1(x^0, c, p)u^0 = 0$  and  $f_2(x^0, c, p) + g_2(x^0, c, p)u^0 = 0$ . The derivative of the output is given by

$$\dot{\bar{y}} = [f_1(\bar{x} + x^0, c, p) + g_1(\bar{x} + x^0, c, p)u^0] + g_1(\bar{x} + x^0, c, p)\bar{u}.$$

Since we know  $g_1(\bar{x} + x^0, c, p) > 0$  for all  $x, c, p$ , the engine has relative degree one. To characterize the zero dynamics, restrict  $x$  to

$$z^* = \{x \in S_x : \psi_1(x) = \xi_1 = \bar{x}_1 = 0\}$$

and take

$$u = u^*(x) = \frac{-f_1(\bar{x} + x^0, c, p) - g_1(\bar{x} + x^0, c, p)u^0 + k\bar{x}_1}{g_1(\bar{x} + x^0, c, p)}$$

we have

$$\begin{aligned} \dot{\bar{x}}_2 &= f_0(0, \bar{x}_2) \\ &= [f_2(x_1^0, \bar{x}_2 + x_2^0, c, p) + g_2(x_1^0, \bar{x}_2 + x_2^0, c, p)u^0] \\ &\quad + \frac{g_2(x_1^0, \bar{x}_2 + x_2^0, c, p)}{g_1(x_1^0, \bar{x}_2 + x_2^0, c, p)} [-f_1(x_1^0, \bar{x}_2 + x_2^0, c, p) \\ &\quad - g_1(x_1^0, \bar{x}_2 + x_2^0, c, p)u^0]. \end{aligned}$$

Now we can study the zero dynamics of the system from the above equation. Notice that

$$\begin{aligned} & \underline{f}_1(x_1^0, \bar{x}_2 + x_2^0, c_i, p_i) \\ &= \frac{\sum_{j=1}^R [a_{j,0}^1(c_i, p_i) + a_{j,1}^1(c_i, p_i)x_1^0] \underline{\mu}_j(x_1^0)}{\sum_{j=1}^R \underline{\mu}_j(x_1^0)} \\ &\quad + \frac{\sum_{j=1}^R a_{j,2}^1(c_i, p_i)(\bar{x}_2 + x_2^0) \underline{\mu}_j(x_1^0)}{\sum_{j=1}^R \underline{\mu}_j(x_1^0)} \\ &= \underline{f}_1(x_1^0, x_2^0, c_i, p_i) + \beta_i^1(x_1^0, c_i, p_i) \bar{x}_2 \\ & \quad f_1(x_1^0, \bar{x}_2 + x_2^0, c, p) \end{aligned}$$

$$\begin{aligned}
&= \frac{\sum_{i=1}^N [f_1(x_1^0, \bar{x}_2 + x_2^0, c_i, p_i)] \mu_i(c, p)}{\sum_{i=1}^N \mu_i(c, p)} \\
&= f_1(x_1^0, x_2^0, c, p) + \beta_1(x_1^0, c, p) \bar{x}_2 \\
g_1(x_1^0, \bar{x}_2 + x_2^0, c_i, p_i) \\
&= \frac{\sum_{j=1}^R a_{j,3}^1(c_i, p_i) \underline{\mu}_j(x_1^0)}{\sum_{j=1}^R \underline{\mu}_j(x_1^0)} \\
&= g_1(x_1^0, c_i, p_i) = \alpha_i^1(x_1^0, c_i, p_i) \\
g_1(x_1^0, \bar{x}_2 + x_2^0, c, p) \\
&= \frac{\sum_{i=1}^N [g_1(x_1^0, \bar{x}_2 + x_2^0, c_i, p_i)] \mu_i(c, p)}{\sum_{i=1}^N \mu_i(c, p)} \\
&= g_1(x_1^0, c, p) = \alpha_1(x_1^0, c, p)
\end{aligned}$$

and, similarly

$$\begin{aligned}
f_2(x_1^0, \bar{x}_2 + x_2^0, c, p) &= f_2(x_1^0, x_2^0, c, p) + \beta_2(x_1^0, c, p) \bar{x}_2 \\
g_2(x_1^0, \bar{x}_2 + x_2^0, c, p) &= g_2(x_1^0, c, p) = \alpha_2(x_1^0, c, p)
\end{aligned}$$

so that we have

$$\begin{aligned}
\dot{\bar{x}}_2 &= f_0(0, \bar{x}_2) \\
&= [f_2(x_1^0, x_2^0, c, p) + \beta_2(x_1^0, c, p) \bar{x}_2 + g_2(x_1^0, c, p) u^0] \\
&\quad + \frac{\alpha_2(x_1^0, c, p)}{\alpha_1(x_1^0, c, p)} [-f_1(x_1^0, x_2^0, c, p) - \beta_1(x_1^0, c, p) \bar{x}_2 \\
&\quad \quad - g_1(x_1^0, c, p) u^0] \\
&= \beta_2(x_1^0, c, p) \bar{x}_2 - \frac{\alpha_2(x_1^0, c, p)}{\alpha_1(x_1^0, c, p)} \beta_1(x_1^0, c, p) \bar{x}_2 \\
&= \left( \beta_2(x_1^0, c, p) - \frac{\alpha_2(x_1^0, c, p)}{\alpha_1(x_1^0, c, p)} \beta_1(x_1^0, c, p) \right) \bar{x}_2.
\end{aligned}$$

Since we know that  $a_{j,3}^1(c_i, p_i) > a_{j,3}^2(c_i, p_i) > 0$  and  $a_{j,2}^2(c_i, p_i) < a_{j,2}^1(c_i, p_i) < 0$  for any  $i = 1, 2, \dots, N, j = 1, 2, \dots, R$ , we have

$$\frac{\sum_{j=1}^R a_{j,3}^1(c_i, p_i) \underline{\mu}_j(x_1^0)}{\sum_{j=1}^R \underline{\mu}_j(x_1^0)} > \frac{\sum_{j=1}^R a_{j,3}^2(c_i, p_i) \underline{\mu}_j(x_1^0)}{\sum_{j=1}^R \underline{\mu}_j(x_1^0)} > 0$$

that is  $\alpha_i^1(x_1^0, c_i, p_i) > \alpha_i^2(x_1^0, c_i, p_i) > 0$  and

$$\frac{\sum_{i=1}^N \alpha_i^1(x_1^0, c_i, p_i) \mu_i(c, p)}{\sum_{i=1}^N \mu_i(c, p)} > \frac{\sum_{i=1}^N \alpha_i^2(x_1^0, c_i, p_i) \mu_i(c, p)}{\sum_{i=1}^N \mu_i(c, p)} > 0$$

that is  $\alpha_1(x_1^0, c, p) > \alpha_2(x_1^0, c, p) > 0$  so that  $0 < \alpha_2(x_1^0, c, p)/\alpha_1(x_1^0, c, p) < 1$ . Also, notice that

$$\begin{aligned}
&\beta_i^2(x_1^0, c, p) - \frac{\alpha_2(x_1^0, c, p)}{\alpha_1(x_1^0, c, p)} \beta_i^1(x_1^0, c, p) \\
&= \frac{\sum_{j=1}^R a_{j,2}^2(c_i, p_i) \underline{\mu}_j(x_1^0)}{\sum_{j=1}^R \underline{\mu}_j(x_1^0)} - \frac{\alpha_2(x_1^0, c, p)}{\alpha_1(x_1^0, c, p)} \\
&\quad \cdot \frac{\sum_{j=1}^R a_{j,2}^1(c_i, p_i) \underline{\mu}_j(x_1^0)}{\sum_{j=1}^R \underline{\mu}_j(x_1^0)} \\
&= \frac{\sum_{j=1}^R \left[ a_{j,2}^2(c_i, p_i) - \frac{\alpha_2(x_1^0, c, p)}{\alpha_1(x_1^0, c, p)} a_{j,2}^1(c_i, p_i) \right] \underline{\mu}_j(x_1^0)}{\sum_{j=1}^R \underline{\mu}_j(x_1^0)}
\end{aligned}$$

$$\begin{aligned}
&< \frac{\sum_{j=1}^R [a_{j,2}^2(c_i, p_i) - a_{j,2}^1(c_i, p_i)] \underline{\mu}_j(x_1^0)}{\sum_{j=1}^R \underline{\mu}_j(x_1^0)} \\
&< 0
\end{aligned}$$

so that

$$\begin{aligned}
&\beta_2(x_1^0, c, p) - \frac{\alpha_2(x_1^0, c, p)}{\alpha_1(x_1^0, c, p)} \beta_1(x_1^0, c, p) \\
&= \frac{\sum_{i=1}^N \beta_i^2(x_1^0, c, p) \mu_i(c, p)}{\sum_{i=1}^N \mu_i(c, p)} \\
&\quad - \frac{\alpha_2(x_1^0, c, p)}{\alpha_1(x_1^0, c, p)} \frac{\sum_{i=1}^N \beta_i^1(x_1^0, c, p) \mu_i(c, p)}{\sum_{i=1}^N \mu_i(c, p)}
\end{aligned}$$

$$= \frac{\sum_{i=1}^N \left[ \beta_i^2(x_1^0, c, p) - \frac{\alpha_2(x_1^0, c, p)}{\alpha_1(x_1^0, c, p)} \beta_i^1(x_1^0, c, p) \right] \mu_i(c, p)}{\sum_{i=1}^N \mu_i(c, p)} < 0.$$

Therefore, the origin of  $\ddot{x}_2 = f_0(0, \bar{x}_2)$  is exponentially stable.

To show that the external part  $\xi$  is stabilized by the control  $u$ , consider the following Lyapunov function candidate [34]:

$$V_i = \frac{1}{2} e_s^2 + \frac{1}{2} \tilde{\theta}_\alpha^\top Q_\alpha \tilde{\theta}_\alpha + \frac{1}{2} \tilde{\theta}_\beta^\top Q_\beta \tilde{\theta}_\beta \quad (45)$$

which quantifies both errors in tracking and in parameter estimation. Using vector derivatives and following [34], the time derivative of (45) is

$$\dot{V}_i = e_s \dot{e}_s + \tilde{\theta}_\alpha^\top Q_\alpha \dot{\tilde{\theta}}_\alpha + \tilde{\theta}_\beta^\top Q_\beta \dot{\tilde{\theta}}_\beta. \quad (46)$$

Note that  $\bar{e}_s(t) = \dot{e}_s(t) - e^{(d)}(t)$  and the  $d$ th derivative of the output error is  $e^{(d)} = y_m^{(d)} - y^{(d)}$  so that

$$\dot{e}_s(t) = \bar{e}_s(t) + y_m^{(d)} - y^{(d)} \quad (47)$$

and from (14), (26), (28), and (27)

$$\begin{aligned} \dot{e}_s(t) &= \bar{e}_s(t) + [\nu(t) - \eta e_s - \bar{e}_s] \\ &\quad - [(\alpha_k(t) + \alpha(x)) + (\beta_k(t) + \beta(x))(u_{ce} + u_{si})] \\ &= -\eta e_s + [\nu(t) - \alpha_k(t) - (\beta_k(t) + \hat{\beta}(x))u_{ce}] \\ &\quad - \alpha(x) + (\hat{\beta}(x) - \beta(x))u_{ce} - (\beta_k(t) + \beta(x))u_{si} \\ &= -\eta e_s + [\nu(t) - \alpha_k(t) + (\alpha_k(t) + \hat{\alpha}(x)) - \nu(t)] \\ &\quad - \alpha(x) + (\hat{\beta}(x) - \beta(x))u_{ce} - (\beta_k(t) + \beta(x))u_{si} \\ &= -\eta e_s + (\hat{\alpha}(x) - \alpha(x)) + (\hat{\beta}(x) - \beta(x))u_{ce} \\ &\quad - (\beta_k(t) + \beta(x))u_{si} \end{aligned}$$

also from (15) to (18), and (23), (24) we have

$$\begin{aligned} \dot{e}_s &= -\eta e_s + (\tilde{\theta}_\alpha^\top \phi_\alpha(x) - \omega_\alpha(x)) + (\tilde{\theta}_\beta^\top \phi_\beta(x) - \omega_\beta(x))u_{ce} \\ &\quad - (\beta_k(t) + \beta(x))u_{si}. \end{aligned}$$

Substitute the above equation into (46), and assume that the ideal parameters are constant so that  $\dot{\tilde{\theta}}_\alpha = \dot{\theta}_\alpha$  and  $\dot{\tilde{\theta}}_\beta = \dot{\theta}_\beta$  and substitute (29), (30) into (46)

$$\begin{aligned} \dot{V}_i &= e_s [-\eta e_s + (\tilde{\theta}_\alpha^\top \phi_\alpha(x) - \omega_\alpha(x)) \\ &\quad + (\tilde{\theta}_\beta^\top \phi_\beta(x) - \omega_\beta(x))u_{ce} - (\beta_k(t) + \beta(x))u_{si}] \\ &\quad + \tilde{\theta}_\alpha^\top Q_\alpha [-Q_\alpha^{-1} \phi_\alpha(x) e_s] + \tilde{\theta}_\beta^\top Q_\beta [-Q_\beta^{-1} \phi_\beta(x) e_s u_{ce}] \\ &= -\eta e_s^2 - (\omega_\alpha(x) + \omega_\beta(x)u_{ce})e_s - (\beta_k(t) + \beta(x))u_{si}e_s. \end{aligned}$$

Notice that we did not consider a projection modification to the update laws above. Clearly, since  $\theta_\alpha^* \in \Omega_\alpha$  and  $\theta_\beta^* \in \Omega_\beta$ , when the projection is in effect it always results in smaller parameter errors that will decrease  $\dot{V}_i$  so that

$$\dot{V}_i \leq -\eta e_s^2 - (\omega_\alpha(x) + \omega_\beta(x)u_{ce})e_s - (\beta_k(t) + \beta(x))u_{si}e_s.$$

Substitute (31) into the above equation and also notice that  $-(\omega_\alpha(x) + \omega_\beta(x)u_{ce})e_s \leq (|\omega_\alpha(x)| + |\omega_\beta(x)u_{ce}|)|e_s| \leq (W_\alpha(x) + W_\beta(x)|u_{ce}|)|e_s|$  and  $\beta_k(t) + \beta(x) \geq \beta_0$  and  $|e_s| = e_s \text{sgn}(e_s)$  (except at  $e_s = 0$ )

$$\begin{aligned} \dot{V}_i &\leq -\eta e_s^2 + (W_\alpha(x) + W_\beta(x)|u_{ce}|)|e_s| \\ &\quad - (\beta_k(t) + \beta(x)) \left( \frac{(W_\alpha(x) + W_\beta(x)|u_{ce}|)}{\beta_0} \text{sgn}(e_s) \right) e_s \\ &\leq -\eta e_s^2 + (W_\alpha(x) + W_\beta(x)|u_{ce}|)|e_s| \\ &\quad - \frac{(\beta_k(t) + \beta(x))}{\beta_0} (W_\alpha(x) + W_\beta(x)|u_{ce}|)|e_s| \\ &\leq -\eta e_s^2. \end{aligned}$$

Thus,  $\dot{V}_i$  is negative semidefinite which means  $V_i$  is a non-increasing function of time, that is, the measure of the tracking error  $e_s$  is bounded. Notice that  $e_s(s) = L(s)e(s)$  and  $L(s)$  is a stable function with the degree of  $d-1$  we know that the tracking error and its derivatives  $e, \dot{e}, \dots, e^{(d-1)}$  are bounded. Since the reference trajectory  $y_m$  and its derivatives  $\dot{y}_m, \dots, y_m^{(d)}$  are assumed to be bounded, the system output  $y$  and its derivatives  $\dot{y}, \dots, y^{(d)}$  are bounded. Hence,  $\xi$  is bounded and thus  $x$  is bounded.

Besides, the fact that  $\dot{V}_i$  is negative semidefinite also implies that parameter estimations  $\theta_\alpha$  and  $\theta_\beta$  are bounded [noting (23), (24) and the boundedness of  $\theta_\alpha^*$  and  $\theta_\beta^*$ ]. Therefore, the boundedness of  $\hat{\alpha}(x)$ ,  $\hat{\beta}(x)$ ,  $\alpha_k(t)$ , and  $\beta_k(t)$  assures that  $u_{ce}$  and  $u_{si}$  and hence  $u$  are bounded.

To show asymptotic stability of the output, note that

$$\int_0^\infty \eta e_s^2 dt \leq - \int_0^\infty \dot{V}_i dt = V_i(0) - V_i(\infty) \quad (48)$$

this establishes that  $e_s \in L_2$  ( $L_2 = \{z(t) : \int_0^\infty z^2(t) < \infty\}$ ) since  $V_i(0)$  and  $V_i(\infty)$  are bounded. Since  $e_s$  and  $\dot{e}_s$  are bounded and  $e_s \in L_2$ , by Barbalat's Lemma we have asymptotic stability of  $e_s$  (i.e.,  $\lim_{t \rightarrow \infty} e_s = 0$ ), which implies asymptotic stability of the tracking error  $e$  (i.e.,  $\lim_{t \rightarrow \infty} e = 0$ ).

### C. Direct Adaptive Control

In addition to the assumptions we made in the indirect adaptive control case, we require  $\beta_k(t) = \alpha_k(t) = 0$  for all  $t \geq 0$ , and that there exist positive constants  $\beta_0$  and  $\beta_1$  such that  $0 < \beta_0 \leq \beta(x) \leq \beta_1$ . Also, we assume that we can specify some function  $B(x) \geq 0$  such that

$$|\dot{\beta}(x)| = \left| \left( \frac{\partial \beta}{\partial x} \right)^\top \dot{x} \right| \leq B(x)$$

for all  $x \in S_x$ . [For our engine application, we will use analytical studies of the model to find  $\beta_0$ ,  $\beta_1$ , and  $B(x)$ .] We know that there exists some ideal controller

$$u^* = \frac{1}{\beta(x)}(-\alpha(x) + \nu(t)) \quad (49)$$

where  $\nu(t)$  is defined the same as in the indirect adaptive control case. Let

$$u^* = \theta_u^{*\top} \phi_u(x, \nu) + u_k(t) + \omega_u(x, \nu) \quad (50)$$

where  $u_k$  is a known part of the controller (e.g., one that was designed for the nominal system without fault) and

$$\theta_u^* = \arg \min_{\theta_u \in \Omega_u} \left( \sup_{x \in S_x, \nu \in S_\nu} |\theta_u^\top \phi_u(x, \nu) - (u^* - u_k)| \right)$$

so that  $\omega_u(x, \nu)$  is the approximation error. We assume that  $|\omega_u(x, \nu)| \leq W_u(x, \nu)$ , where  $W_u(x, \nu)$  is a known bound on the error in representing the ideal controller. The approximation of the ideal controller may be represented by

$$\hat{u} = \theta_u^\top \phi_u(x, \nu) + u_k(t) \quad (51)$$

where the parameter vector  $\theta_u(t)$  is updated on line and the parameter error is

$$\tilde{\theta}_u(t) = \theta_u(t) - \theta_u^*. \quad (52)$$

Consider the direct adaptive control law

$$u = \hat{u} + u_{sd} \quad (53)$$

which is the sum of the approximation to the ideal control law and a sliding mode control term

$$u_{sd} = \left( \frac{B(x)|e_s|}{2\beta_0^2} + W_u(x, \nu) \right) \text{sgn}(e_s) \quad (54)$$

and we use the update law

$$\dot{\theta}_u(t) = Q_u^{-1} \phi_u(x, \nu) e_s(t) \quad (55)$$

where  $Q_u$  is positive definite and diagonal. We also use a projection method to ensure that  $\theta_u \in \Omega_u$ .

Consider the following Lyapunov function candidate

$$V_d = \frac{1}{2\beta(x)} e_s^2 + \frac{1}{2} \tilde{\theta}_u^\top Q_u \tilde{\theta}_u \quad (56)$$

taking the time derivative

$$\dot{V}_d = \frac{e_s}{\beta(x)} \dot{e}_s - \frac{\dot{\beta}(x) e_s^2}{2\beta^2(x)} + \tilde{\theta}_u^\top Q_u \dot{\tilde{\theta}}_u. \quad (57)$$

Note that  $\bar{e}_s(t) = \dot{e}_s(t) - e^{(d)}(t)$  and the  $d$ th derivative of the output error is  $e^{(d)} = y_m^{(d)} - y^{(d)}$  so that

$$\dot{e}_s(t) = \bar{e}_s(t) + y_m^{(d)} - y^{(d)} \quad (58)$$

and from (14), (28), (53), and (49) and by assuming  $\alpha_k(t) = \beta_k(t) = 0$

$$\begin{aligned} \dot{e}_s(t) &= \bar{e}_s(t) + [\nu(t) - \eta e_s - \bar{e}_s] \\ &\quad - [(\alpha_k(t) + \alpha(x)) + (\beta_k(t) + \beta(x))(\hat{u} + u_{sd})] \\ &= -\eta e_s + [\nu(t) - \alpha(x) - \beta(x)u^*] \\ &\quad - \beta(x)(\hat{u} - u^*) - \beta(x)u_{sd} \\ &= -\eta e_s - \beta(x)(\hat{u} - u^*) - \beta(x)u_{sd} \end{aligned}$$

also from (51), (49), and (52) we have

$$\dot{e}_s(t) = -\eta e_s - \beta(x)(\tilde{\theta}_u^\top \phi_u(x, \nu) - \omega_u(x, \nu)) - \beta(x)u_{sd}.$$

Substitute the above equation into (57), and assume that the ideal parameters are constant so that  $\dot{\theta}_u = \dot{\tilde{\theta}}_u$  and substitute (55) into (57)

$$\begin{aligned} \dot{V}_d &= \frac{e_s}{\beta(x)} [-\eta e_s - \beta(x)(\tilde{\theta}_u^\top \phi_u(x, \nu) - \omega_u(x, \nu)) - \beta(x)u_{sd}] \\ &\quad - \frac{\dot{\beta}(x) e_s^2}{2\beta^2(x)} + \tilde{\theta}_u^\top Q_u [Q_u^{-1} \phi_u(x, \nu) e_s(t)] \\ &= -\frac{\eta e_s^2}{\beta(x)} - \left( \tilde{\theta}_u^\top \phi_u - \omega_u(x, \nu) + \frac{\dot{\beta}(x) e_s}{2\beta^2(x)} - \tilde{\theta}_u^\top \phi_u \right) e_s \\ &\quad - e_s u_{sd} \\ &= -\frac{\eta e_s^2}{\beta(x)} - \left( \frac{\dot{\beta}(x) e_s}{2\beta^2(x)} - \omega_u(x, \nu) \right) e_s - e_s u_{sd}. \end{aligned}$$

After we consider the projection modification to the update law we have

$$\dot{V}_d \leq -\frac{\eta e_s^2}{\beta(x)} - \left( \frac{\dot{\beta}(x) e_s}{2\beta^2(x)} - \omega_u(x, \nu) \right) e_s - e_s u_{sd}. \quad (59)$$

Substitute (54) into the above equation and notice that

$$\begin{aligned} &- \left( \frac{\dot{\beta}(x) e_s}{2\beta^2(x)} - \omega_u(x, \nu) \right) e_s \\ &\leq \left( \frac{|\dot{\beta}(x)| |e_s|}{2\beta^2(x)} + |\omega_u(x, \nu)| \right) |e_s| \\ &\leq \left( \frac{B(x) |e_s|}{2\beta_0^2(x)} + W_u(x, \nu) \right) |e_s| \end{aligned}$$

and  $0 < \beta_0 \leq \beta(x) \leq \beta_1$  we have

$$\dot{V}_d \leq -\frac{\eta e_s^2}{\beta(x)} \quad (60)$$

so that  $V_d$  is a nonincreasing function of time. This gives the same type of stability result that we obtained in the indirect case.

#### IV. COMPONENT LEVEL MODEL SIMULATION

To study the effectiveness of the proposed fault-tolerant control methods, we apply them to the component level model simulation, which we treat as the real application on the XTE46

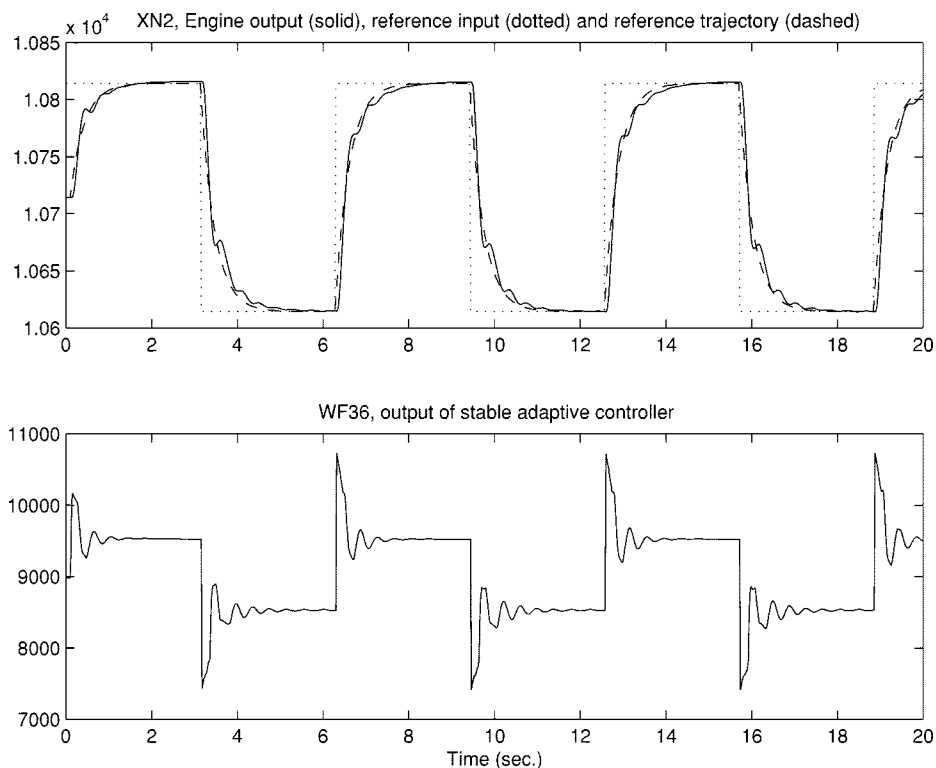


Fig. 3. Performance of indirect adaptive controller for the engine without fault.

engine. Actually, we first applied them to the design model but in the interest of brevity we do not show those (slightly better) results here.

#### A. Indirect Adaptive Control

Consider the engine in the form of

$$\begin{aligned} \dot{y} &= f_1(x, c, p) + g_1(x, c, p)u \\ &= [\alpha_k(c, p_0, t) + \alpha(x, c, p)] + [\beta_k(c, p_0, t) + \beta(x, c, p)]u \end{aligned}$$

where  $y = x_1$ . Since  $g_1(x, c, p) > 0$  for any  $x, c, p$ , the relative degree of the engine is one. Furthermore, by studying the dynamics of the developed nonlinear model we know that  $g_1(x, c, p) > 0.32$  so that we can set  $\beta_0 = 0.32$ . We use our developed engine model to represent the nominal model dynamics  $\alpha_k(c, p_0, t)$  and  $\beta_k(c, p_0, t)$  by setting the quality parameters to be the nominal value  $p_0$ . The unknown dynamics  $\alpha(x, c, p)$  and  $\beta(x, c, p)$  describe both the model uncertainty caused by nominal model inaccuracy and system changes due to fault effects. They will be approximated by two Takagi–Sugeno fuzzy systems  $\hat{\alpha}$  and  $\hat{\beta}$  with  $R = 11$  rules for each. The inputs to the fuzzy systems include two state variables and the parameters are updated online to capture the unknown dynamics affected by model inaccuracy and faults so that fault tolerance can be achieved. Note that the stable adaptive controller will ensure the stability of  $x_1$ , and the exponential attractivity of the engine zero dynamics will ensure the stability of the unobservable state  $x_2$ . Since the relative degree of the system is one, the error dynamics are simple ( $e_s(t) = e(t)$  and  $\bar{e}_s(t) = 0$ ).

Note that the sliding mode control term can introduce a high frequency signal to the plant which may excite unmodeled dy-

namics. To avoid this, we use a “smoothed” sliding mode control term

$$u_{si} = \frac{(W_\alpha(x) + W_\beta(x)|u_{ce}|)}{\beta_0} \text{sat}(e_s/\epsilon) \quad (61)$$

where  $\epsilon > 0$  and

$$\text{sat}(x) = \begin{cases} 1, & \text{if } x \geq 1 \\ x, & \text{if } -1 < x < 1 \\ -1, & \text{if } x \leq -1. \end{cases} \quad (62)$$

By using this smoothed control action the tracking error will converge asymptotically to an  $\epsilon$ -neighborhood of  $e = 0$  [34]. Taking into account of the engine dynamics, the model uncertainty is described by  $W_\alpha = 0.01$  and  $W_\beta = 0.01$ , the adaptation gains are  $Q_\alpha^{-1} = 5e - 8$  and  $Q_\beta^{-1} = 1e - 17$ , and the design parameters are chosen to be  $\eta = 1$  and  $\epsilon = 10$ .

We let the CLM run at the operating condition of ALT = 15000, XM = 0.7, DTAMB = 0, and PC = 46. For quality parameters of the engine, we set the initial engine variation to be  $p_{iev} = [0.1\%, 0.1\%, 0.2\%, 0.1\%, -0.1\%, 0, -0.3\%, 0.2\%, -0.1\%, 0.1\%]$ , and the engine deterioration index to be 0.1. The reference trajectory is defined by passing a square wave through a linear reference model  $Y_m(s)/R(s) = 3/s + 3$ . The control performance for an engine without any fault ( $p_f = 0$ ) is shown in Fig. 3 and Fig. 4 shows the control result for an engine with large fan fault ( $p_{f,ZSW2} = -3\%$  and  $p_{f,SEDM2} = -3\%$ ), which is introduced in the beginning of the simulation as an abrupt-type fault. The indirect adaptive controller is able to quickly control the engine even in the presence of a large fan fault. This is because the controller can take advantage of

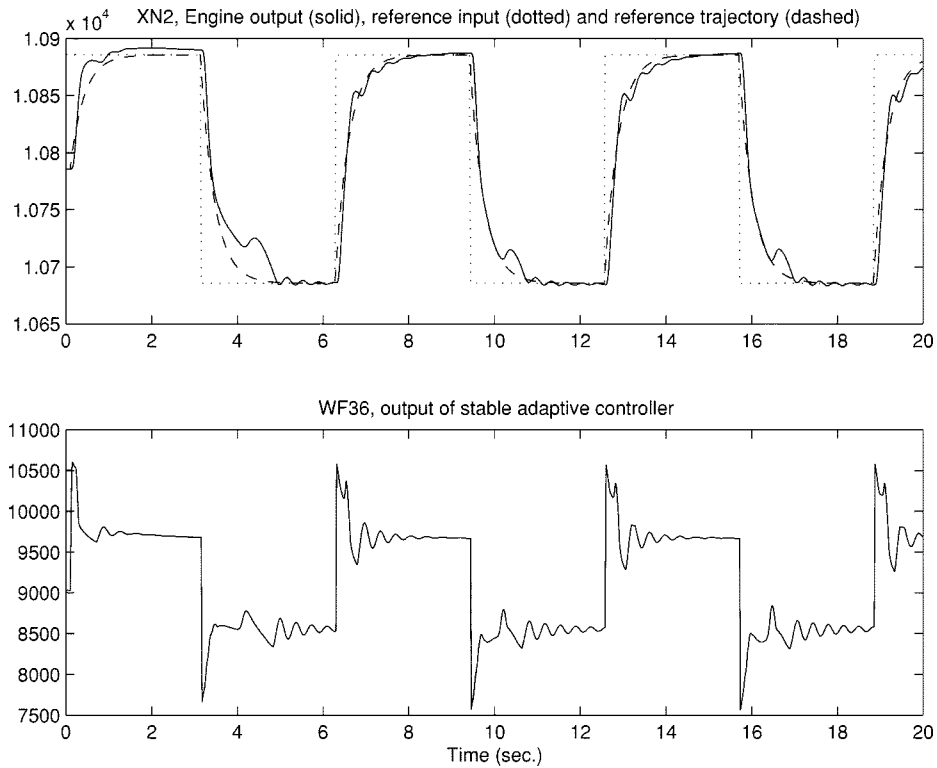


Fig. 4. Performance of indirect adaptive controller for the engine with large fan fault.

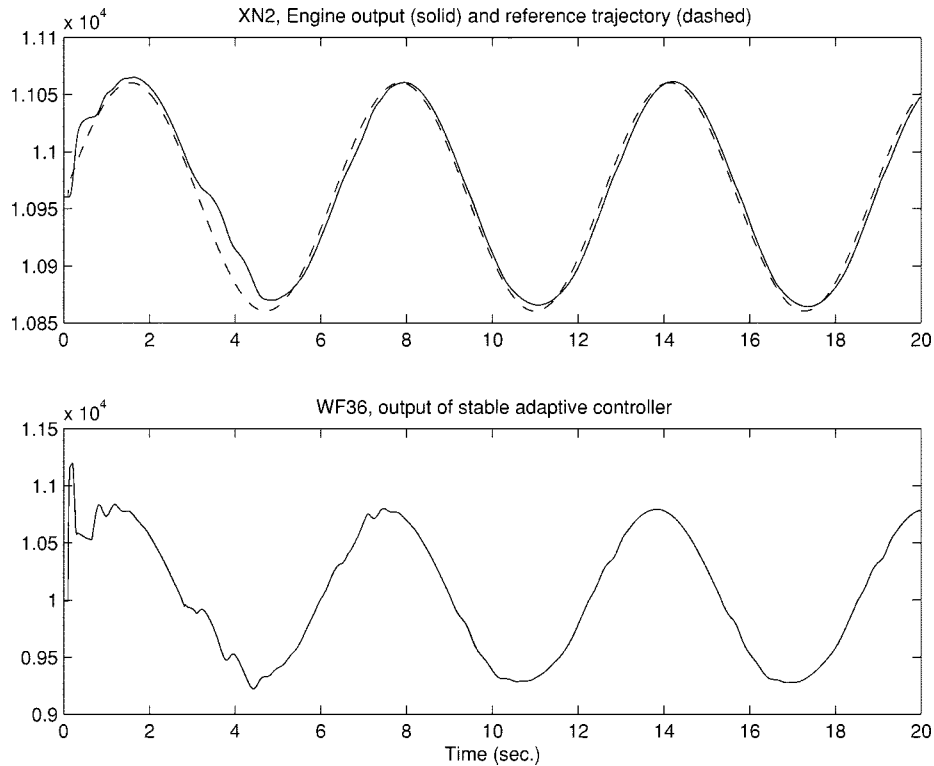


Fig. 5. Performance of indirect adaptive controller for the engine with small fan fault and medium compressor hub fault (sine input).

the nominal model to have *a priori* knowledge of the engine, and its adaption scheme can let fuzzy approximators learn the profile of faults so that the control action can be modified to accommodate the fault. Notice that there is some small oscillation caused by parameter updates and there is a small ripple for

the large fan fault case which implies that there may exist some high-frequency dynamics that can not be learned by the approximator.

We also studied the performance for sine inputs (and many other cases). This time we let the CLM run at a different oper-

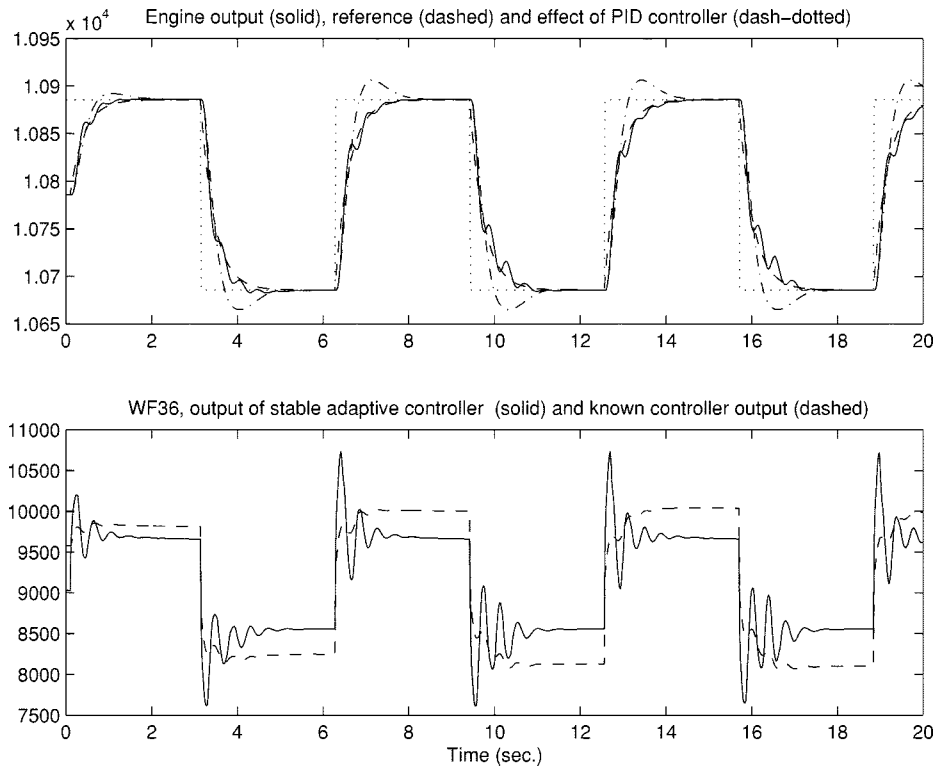


Fig. 6. Performance of direct adaptive controller and PI controller for the engine with large fan fault.

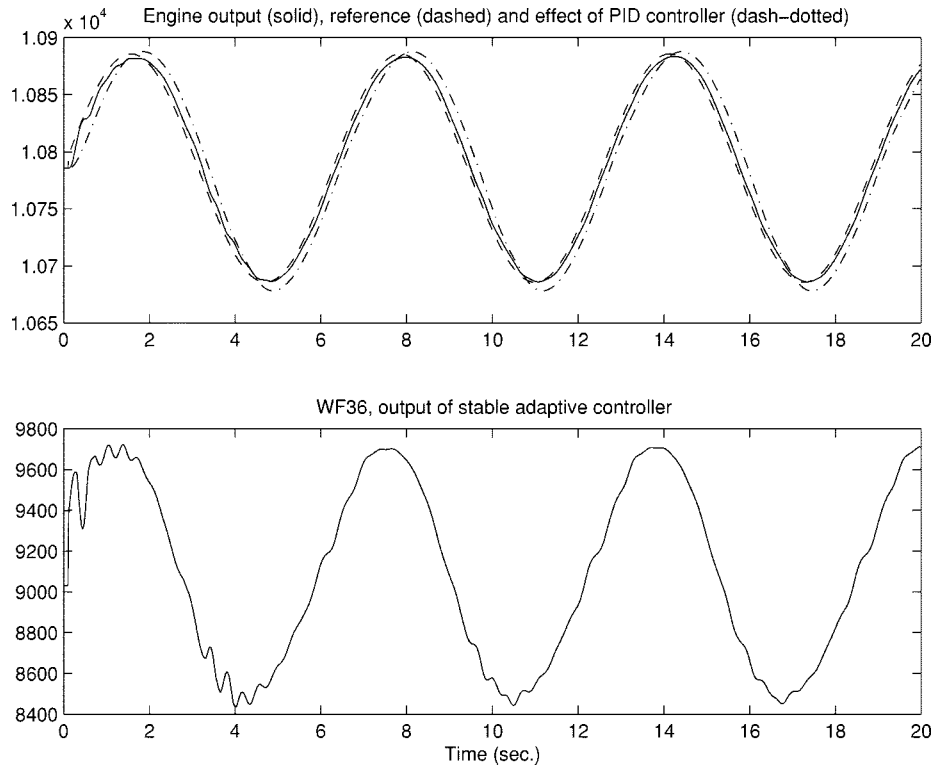


Fig. 7. Performance of direct adaptive controller and PI controller for the engine with large fan fault (sine input).

ating condition ( $ALT = 16000$ ,  $XM = 0.72$ ,  $DTAMB = 0$ , and  $PC = 49$ ), the initial engine variation be  $p_0 = [0.2\%, 0.1\%, 0.3\%, 0.1\%, -0.1\%, 0, -0.3\%, 0.2\%, -0.1\%, 0.1\%]$ , and the engine deterioration index be 0.3. The control performance for an engine with a small fan fault ( $p_{f,ZSW2} = -1\%$

and  $p_{f,SEDM2} = -1\%$ ) and a medium compressor hub fault ( $p_{f,ZSW27} = -2\%$  and  $p_{f,SEDM27} = -2\%$ ) is shown in Fig. 5, which is also introduced in the beginning of the simulation as abrupt changes. Note that in the first 5 seconds the adaptation scheme operates actively to learn the characteristics of the large

fan fault. Afterwards, there is little adaptation and the control is quite smooth.

### B. Direct Adaptive Control

We will now show how to apply the direct adaptive control scheme to the fault-tolerant engine control problem. For direct adaptive control scheme, the nominal engine model cannot be used. Instead, we define the known controller to be a proportional-integral (PI) controller ( $u_k = k_p(e + 1/T_i \int edt)$ ,  $k_p = 5$ ,  $T_i = 0.2$ ). By studying dynamics of the developed nonlinear model we also know that  $g_1(x, c, p) < 0.38$  and its rate of change is smaller than 1.5 so that we can set  $\beta_1 = 0.38$  and  $B = 1.5$ . We also use a smoothed sliding mode control term here and the model uncertainty is described by  $W_u = 200$ , the adaptation gain is  $Q_u^{-1} = 2e - 7$  and the design parameters are chosen to be  $\eta = 1$  and  $\epsilon = 10$ .

We try to compare the control result of the indirect adaptive controller with that of the direct adaptive controller, in particular, the large fan fault case as shown in Fig. 4. The direct adaptive control result is shown in Fig. 6. Note that there is more oscillation in the direct case. This is because the direct adaptive controller can not use *a priori* knowledge of the engine from the nominal engine model. Instead, it uses a known controller (its effect is shown in the figure using dashed line), which does not perform as well, so that the control action more heavily relies on the adaptation scheme. It is also interesting to compare the control result of the stable adaptive controller with that of a PI controller, tuned by the Ziegler-Nichols technique. (Note that the PI controller is not gain scheduled since we only compare the performance at one operating point.) There is large overshoot caused by the change of system dynamics and the PI controller, of course, is unable to "learn" it. We may expect more performance deterioration for the PI controller when the fault is more serious, while the fault-tolerant engine controller may recover from it. Similar studies have been performed for the sine input case, as shown in Fig. 7 (and many other cases). The direct adaptive controller can learn the change of system dynamics quickly. For the PI controller, there is a large residual.

## V. CONCLUSION

Stable indirect and direct adaptive controllers are applied to achieve fault-tolerant engine control by using Takagi-Sugeno fuzzy systems to "learn" the unknown dynamics caused by faults and to accommodate faults by updating the controller. By developing the analytical model and studying system zero dynamics, we prove that both adaptive schemes achieve asymptotic tracking results. The performance of the fault-tolerant indirect and direct adaptive controller is also demonstrated through the component level model simulation of the XTE46 engine.

## ACKNOWLEDGMENT

The authors would like to thank Dr. S. Adibhatla at General Electric Aircraft Engines for providing the CLM for the engine, technical advice on how to use it, and feedback on the development of the modeling and control strategies. Moreover, we

would like to thank T. H. Guo at NASA Glenn Research Center for his support.

## REFERENCES

- [1] R. J. Patton, "Fault-tolerant control: The 1997 situation," in *IFAC Fault Detection, Supervision and Safety for Technical Processes*, Kingston Upon Hull, U.K., 1997, pp. 1029-1051.
- [2] R. F. Stengel, "Intelligent failure-tolerant control," *IEEE Contr. Syst. Mag.*, vol. 11, pp. 14-23, June 1991.
- [3] W. C. Merrill, "Sensor failure detection for jet engines using analytical redundancy," *J. Guidance, Contr., Dyn.*, vol. 8, no. 6, pp. 673-682, 1985.
- [4] W. C. Merrill, J. C. DeLaat, and W. M. Bruton, "Advanced detection, isolation, and accommodation of sensor failures—A real-time evaluation," *J. Guidance, Contr., Dyn.*, vol. 11, no. 6, pp. 517-526, 1988.
- [5] W. C. Merrill, J. C. DeLaat, and M. Abdelwahab, "Turbofan engine demonstration of sensor failure-detection," *J. Guidance, Contr., Dyn.*, vol. 14, no. 2, pp. 337-349, 1991.
- [6] A. Duyar and W. C. Merrill, "Fault diagnosis for the space shuttle main engine," *J. Guidance, Contr., Dyn.*, vol. 15, no. 2, pp. 384-389, 1992.
- [7] A. Duyar, V. Eldem, W. C. Merrill, and T. H. Guo, "Fault detection and diagnosis in propulsion systems—A fault parameter estimation approach," *J. Guidance, Contr., Dyn.*, vol. 17, no. 1, pp. 104-108, 1994.
- [8] R. J. Patton and J. Chen, "Robust fault detection of jet engine sensor systems using eigenstructure assignment," *J. Guidance, Contr., Dyn.*, vol. 15, no. 6, pp. 1491-1497, 1992.
- [9] R. J. Patton, J. Chen, and H. Y. Zhang, "Observer-based fault detection and isolation: Robustness and applications," *Contr. Eng. Practice*, vol. 5, no. 5, pp. 671-682, 1997.
- [10] R. J. Patton and J. Chen, "Modeling methods for improving robustness in fault diagnosis of jet engine system," in *Proc. 31st IEEE Conf. Contr. Decision*, Tucson, AZ, 1997, pp. 2330-2335.
- [11] T. E. Menke and P. S. Maybeck, "Sensor/actuator failure-detection in the vista F-16 by multiple model adaptive estimation," *IEEE Trans. Aerospace Electronic Syst.*, vol. 31, no. 4, pp. 1218-1229, 1995.
- [12] P. S. Maybeck and R. D. Stevens, "Reconfigurable flight control via multiple model adaptive control methods," *IEEE Trans. Aerospace Electron. Syst.*, pp. 470-479, 1991.
- [13] M. Athans, D. Castanon, K. Dunn, C. S. Greene, W. H. Lee, N. R. Sandell, and A. S. Willsky, "The stochastic control of the F-8C aircraft using a multiple model adaptive control (MMAC) method—Part 1: Equilibrium flight," *IEEE Trans. Automat. Contr.*, vol. 22, pp. 768-780, 1977.
- [14] W. D. Morse and K. A. Ossman, "Model-following reconfigurable flight control system for the AFTI/F-16," *J. Guidance, Contr., Dyn.*, vol. 13, no. 6, pp. 969-976, 1990.
- [15] C. Y. Huang and R. F. Stengel, "Restructurable control using proportional-integral implicit model following," *J. Guidance, Contr., Dyn.*, vol. 13, no. 2, pp. 303-309, 1990.
- [16] Y. Ochi and K. Kanai, "Design of restructurable flight control systems using feedback linearization," *J. Guidance, Contr., Dyn.*, vol. 14, no. 5, pp. 903-911, 1991.
- [17] P. J. Antsaklis and K. M. Passino, Eds., *An Introduction to Intelligent and Autonomous Control*. Norwell, MA: Kluwer, 1993.
- [18] R. F. Stengel, "Toward intelligent flight control," *IEEE Trans. Syst., Man, Cybern.*, vol. 23, no. 6, pp. 1699-1717, 1993.
- [19] T. Sorsa, H. N. Koivo, and H. Koivisto, "Neural networks in process fault diagnosis," *IEEE Trans. Syst., Man, Cybern.*, vol. 21, no. 4, pp. 815-825, 1991.
- [20] Y. Maki and K. A. Loparo, "A neural network approach to fault detection and diagnosis in industrial processes," *IEEE Trans. Contr. Syst. Technol.*, vol. 5, pp. 529-541, 1997.
- [21] M. Ayoubi and R. Isermann, "Neuro-fuzzy systems for diagnosis," *Fuzzy Sets Syst.*, vol. 89, no. 3, pp. 289-307, 1997.
- [22] M. M. Polycarpou and A. Vemuri, "Learning methodology for failure detection and accommodation," *IEEE Contr. Syst. Mag.*, vol. 15, pp. 16-24, 1995.
- [23] A. Vemuri and M. M. Polycarpou, "Robust nonlinear fault diagnosis in input-output systems," *Int. J. Contr.*, vol. 68, no. 2, pp. 343-360, 1997.
- [24] M. Demetriou and M. M. Polycarpou, "Incipient fault diagnosis of dynamical systems using on-line approximators," *IEEE Trans. Automat. Contr.*, vol. 43, no. 11, pp. 1612-1617, 1998.
- [25] K. M. Passino and P. J. Antsaklis, "Fault detection and identification in an intelligent restructurable controller," *J. Intell. Robot. Syst.*, vol. 1, pp. 145-161, June 1988.

- [26] E. G. Laukonen, K. M. Passino, V. Krishnaswami, G.-C. Luh, and G. Rizzoni, "Fault detection and isolation for an experimental internal combustion engine via fuzzy identification," *IEEE Trans. Contr. Syst. Technol.*, vol. 3, pp. 347–355, Sept. 1995.
- [27] H. Schneider and P. Frank, "Observer based supervision and fault detection in robots using nonlinear and fuzzy logic residual evaluation," *IEEE Trans. Contr. Syst. Technol.*, vol. 4, no. 3, pp. 274–282, 1996.
- [28] P. M. Frank and B. Koppen-Seliger, "Fuzzy logic and neural network application to fault diagnosis," *Int. J. Approximate Reasoning*, vol. 16, no. 1, pp. 67–88, 1997.
- [29] R. Isermann, "On fuzzy logic applications for automatic control, supervision, and fault diagnosis," *IEEE Trans. Syst., Man, Cybern. Part A*, vol. 28, no. 2, pp. 221–235, 1998.
- [30] —, "Fault diagnosis of machines via parameter estimation and knowledge processing," *Automatica*, vol. 29, pp. 815–836, 1993.
- [31] W. A. Kwong, K. M. Passino, E. G. Laukonen, and S. Yurkovich, "Expert supervision of fuzzy learning systems for fault-tolerant aircraft control," *Proc. IEEE*, pt. Special Issue on Fuzzy Logic in Engineering Applications, vol. 83, pp. 466–483, Mar. 1995.
- [32] S. Adibhatla and T. Lewis, "Model-based intelligent digital engine control," in *AIAA-97-3192, 33rd Joint Propulsion Conf.*, July 1997.
- [33] K. M. Passino and S. Yurkovich, *Fuzzy Control*. Menlo Park, CA: Addison Wesley Longman, 1998.
- [34] H. K. Khalil, *Nonlinear Systems*. New York: MacMillan, Inc., 1996.



**Yixin Diao** received the Bachelor and Master degrees from Tsinghua University, Beijing, China, in 1994 and 1997, respectively, and the Ph.D. degree in electrical engineering from Ohio State University, Columbus in 2000.

Since 2001, he has been with the Performance Management Department at IBM Thomas J. Watson Research Center, Hawthorne, NY. His research interests include intelligent systems and adaptive control.



**Kevin M. Passino** (S'79–M'90–SM'96) received the Ph.D. degree in electrical engineering from the University of Notre Dame, Notre Dame, IN, in 1989.

He has worked on control systems research at Magnavox Electronic Systems Co. and McDonnell Aircraft Co. He spent a year at Notre Dame as a Visiting Assistant Professor and is currently a Professor in the Department of Electrical Engineering at Ohio State University. He has been an Associate Editor for the IEEE TRANSACTIONS ON AUTOMATIC CONTROL and the IEEE TRANSACTIONS ON FUZZY SYSTEMS.

He is Coeditor (with P. J. Antsaklis) of the book *An Introduction to Intelligent and Autonomous Control* (Boston, MA: Kluwer, 1993); coauthor (with S. Yurkovich) of the book *Fuzzy Control* (Menlo Park, CA: Addison Wesley Longman, 1998); coauthor (with K. L. Burgess) of the book *Stability Analysis of Discrete Event Systems* (New York: Wiley, 1998); and coauthor (with V. Gazi, M. L. Moore, W. Shackleford, F. Proctor, and J. S. Albus) of the book *The RCS Handbook: Tools for Real Time Control Systems Software Development* (New York: Wiley, 2001). He has authored more than 130 technical papers and his research interests include intelligent systems and control, adaptive systems, stability analysis, and fault-tolerant control.

Dr. Passino has served as the Vice President of Technical Activities of the IEEE Control Systems Society (CSS); was an elected Member of the IEEE Control Systems Society Board of Governors; was Chair for the IEEE CSS Technical Committee on Intelligent Control; served as the Guest Editor for the 1993 IEEE Control Systems Magazine Special Issue on Intelligent Control; and a Guest Editor for a special track of papers on Intelligent Control for IEEE Expert Magazine in 1996; and was on the Editorial Board of the *International Journal for Engineering Applications of Artificial Intelligence*. He was a Program Chairman for the Eighth IEEE International Symposium on Intelligent Control, 1993 and was the General Chair for the 11th IEEE International Symposium on Intelligent Control. He is the Program Chair of the 2001 IEEE Conference on Decision and Control.